Geophysical Research Letters

RESEARCH LETTER
10.1029/2022GL099419

Special Section:
Southern Ocean and Climate: Biogeochemical and Physical Fluxes and Processes

Modification of North Atlantic Deep Water by Pacific/Upper Circumpolar Deep Water in the Argentine Basin

S. V. S. Brand[1,2], C. J. Prend[1], and L. D. Talley[1]

[1]Scripps Institution of Oceanography, University of California San Diego, La Jolla, CA, USA, [2]University of Rhode Island, Narragansett, RI, USA

Key Points:

- Pacific/Circumpolar Deep Water (CDW) with low oxygen, salinity, and pH dilutes North Atlantic Deep Water (NADW) in the South Atlantic's Argentine Basin
- Isolated low oxygen anomalies in the northwest Argentine Basin indicate a direct path of CDW northward via the Malvinas
- Strong isopycnic temperature variability along the western boundary identifies this as a mixing hotspot for these two deep water masses

Supporting Information:

Supporting Information may be found in the online version of this article.

Correspondence to:

S. V. S. Brand,
svbrand@uri.edu

Citation:

Brand, S. V. S., Prend, C. J., & Talley, L. D. (2023). Modification of North Atlantic Deep Water by Pacific/Upper Circumpolar Deep Water in the Argentine Basin. *Geophysical Research Letters*, *50*, e2022GL099419. https://doi.org/10.1029/2022GL099419

Received 3 MAY 2022
Accepted 1 DEC 2022

Abstract Much of the salty, high oxygen North Atlantic Deep Water (NADW) leaving the Atlantic flows through the Argentine Basin, where it is diluted by fresher, low oxygen Circumpolar Deep Water (CDW). This mixing of deep water masses is often overlooked in the zonally averaged description of the overturning circulation. Here, we show that intense mixing occurs along the western boundary: (a) extreme, isolated oxygen/temperature anomalies recorded by three autonomous biogeochemical floats suggest that subsurface eddies can inject relatively unmodified CDW far into the northwestern Argentine Basin, and (b) moderate, numerous temperature/salinity anomalies indicate a mixing zone from Rio Grande Rise to the Malvinas Current. This western eddy pathway shortcuts the gyre-scale cyclonic route for CDW inferred from most previous studies. Significantly, CDW dilution of NADW affects the properties of deep waters that upwell in the Southern Ocean, and hence the connection between Northern and Southern Hemisphere polar climates.

Plain Language Summary Water, heat, and carbon are transported around the global ocean by the meridional overturning circulation, which helps regulate the climate system. In the Atlantic Ocean, the overturning circulation is characterized by net southward flow in the deep water layers, which transports water from the northern North Atlantic (North Atlantic Deep Water; NADW) all the way to the Southern Ocean. Often neglected in this picture is the modification of these deep waters as they flow south toward the Antarctic. Specifically, they become colder, fresher and less oxygenated due to mixing with much older deep water from the South Pacific, which enters the Atlantic below South America and joins the Circumpolar Deep Water (CDW) flowing northward into the Argentine Basin. Here, using autonomous float measurements, we investigate the mixing between NADW and CDW in the Argentine Basin. We show that isolated boluses of CDW with properties from the Malvinas are found far to the north on the western side of the basin, suggesting transport by isolated subsurface eddies. Understanding these pathways is important because they influence the properties of the water that rises to the surface in the Southern Ocean; dilution of NADW by CDW damps the transmission of Northern Hemisphere climate change to the Southern Ocean.

1. Introduction

The Atlantic Meridional Overturning Circulation (AMOC) plays a key role in the climate system by redistributing heat, salt, and other tracers globally (e.g., McCarthy et al., 2015; Talley et al., 2011). The AMOC "strength" is quantified from the net meridional transport as a function of latitude, subdivided into pressure or isopycnal layers (e.g., Lumpkin & Speer, 2007; Talley et al., 2003). The South Atlantic portion of the AMOC (SAMOC) consists of southward-flowing North Atlantic Deep Water (NADW) balanced by northward-flowing layers above and below—the thermocline/Antarctic Intermediate Water (AAIW)/Upper Circumpolar Deep Water (UCDW), and Lower Circumpolar Deep Water (LCDW)/Antarctic Bottom Water (AABW), respectively (e.g., Ganachaud & Wunsch, 2000; Garzoli & Matano, 2011; Hernandez-Guerra et al., 2019; Lumpkin & Speer, 2007; Schmitz, 1995; Talley et al., 2003; Wüst, 1935).

However, this zonally integrated view of the AMOC obscures significant lateral variations in transport within each layer (e.g., Hernández-Guerra et al., 2019; Reid, 1989). Particularly for the AMOC's intermediate and deep layers, lateral circulation is often neglected despite its role in juxtaposing different water masses and hence modifying their properties. Such exchanges have been articulated and quantified in the North Atlantic as central to the evolution of tracer ages along the Deep Western Boundary Current (DWBC) (Rhein et al., 2015) and at high latitudes (McCartney, 1992).

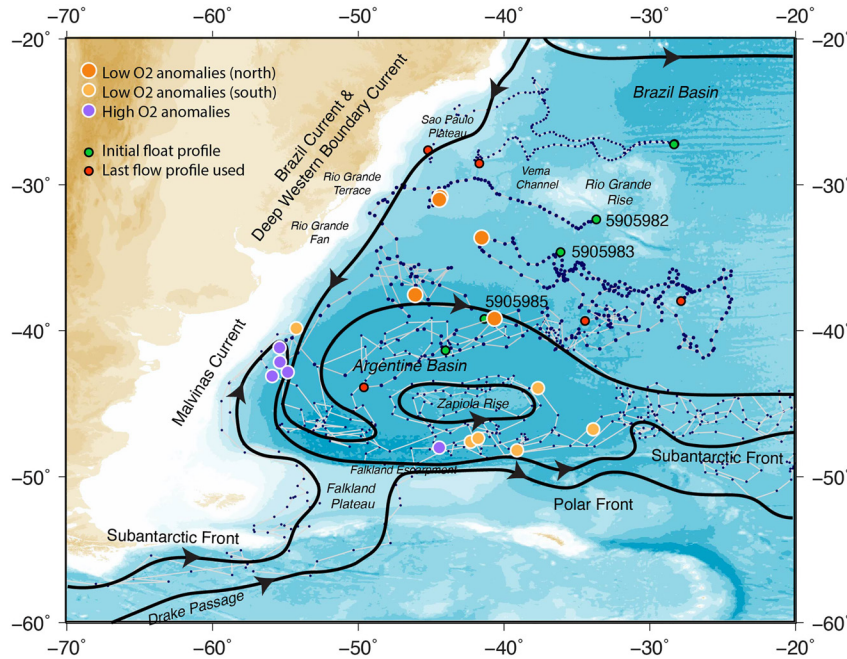

Figure 1. Schematic of Argentine Basin deep water circulation, based in part on Reid (1989) and Valla et al. (2018). White bordered dots: oxygen anomalies measured by Southern Ocean Carbon and Climate Observations and Modeling (SOCCOM) biogeochemical (BGC) Argo floats. Large orange dots: anomalously low oxygen profiles in the northern Argentine Basin (Figure 3). Lighter, smaller orange dots: additional anomalously low oxygen profiles in the southern Argentine Basin. Purple dots: anomalously high oxygen profiles. Profiles from the 5 SOCCOM floats deployed on the RRS James Clark Ross AMT28 expedition in 2018 are shown (medium blue dots; green dots (first profile); red dots (last profile). Profile locations (small blue dots) from 3 other SOCCOM floats deployed in northern Drake Passage and the southeast Pacific are also shown. The profile locations reflect data available through 21 Jan. 2022. See Figures S2 and S4 in Supporting Information S1 for trajectories and oxygen profiles.

Similarly, in the South Atlantic, the net southward transport of "NADW" (potential density range $\sigma_2 = 36.65–36.9$ kg m^{-3}) is more precisely the residual between southward-flowing NADW and northward-flowing Circumpolar Deep Water (CDW) (Georgi, 1981; Reid et al., 1977; Valla et al., 2018). The geostrophic circulation and interleaving of these deep waters were mapped and described by Reid (1989, 1994) (Figure S1b in Supporting Information S1), and are depicted schematically in Figure 1. In the subtropical South Atlantic, NADW first branches eastward from the DWBC in the Brazil Basin but most continues southward into the Argentine Basin before entering the Antarctic Circumpolar Current (ACC) (Garzoli & Matano, 2011; Stramma & England, 1999). Garzoli et al. (2015) calculate that almost 80% of the NADW transport follows the latter pathway through the Argentine Basin, which is consistent with Lagrangian particle release experiments in Tamsitt et al. (2017).

Once in the Argentine Basin, the salty, high oxygen NADW meets CDW that enters from the south via the Malvinas Current, which arises from the Subantarctic Front in Drake Passage (Piola & Gordon, 1989; Stramma & England, 1999) (Figure 1). CDW contains a large component of fresher, low oxygen Pacific Deep Water (PDW) from the southeast Pacific. Abyssal eddies containing relatively unmodified LCDW have been observed from multiple hydrographic surveys in the western Argentine Basin (Arhan et al., 2002; Gordon & Greengrove, 1986) (green squares in Figure 2). The contrast between NADW and CDW has been readily apparent as far back as Wüst (1935) (see Figure S1 in Supporting Information S1) and culminates in a reduction of oxygen in waters identified as NADW in the Argentine Basin (Jullion et al., 2010).

In this study, we use data from core and biogeochemical (BGC) Argo floats to reassess the interaction between NADW and CDW in the SAMOC. We find isolated anomalies of oxygen, temperature, and salinity in the deep water density range that indicate penetration of unmixed CDW far into the northern Argentine Basin. While vigorous eddies are found throughout the region (e.g., Mason et al., 2017), mixing between NADW and CDW occurs primarily along the western boundary, where the water masses meet and their contrast is greatest. This dilution of NADW by CDW is more than a regional curiosity; when NADW reaches the Southern Ocean, it

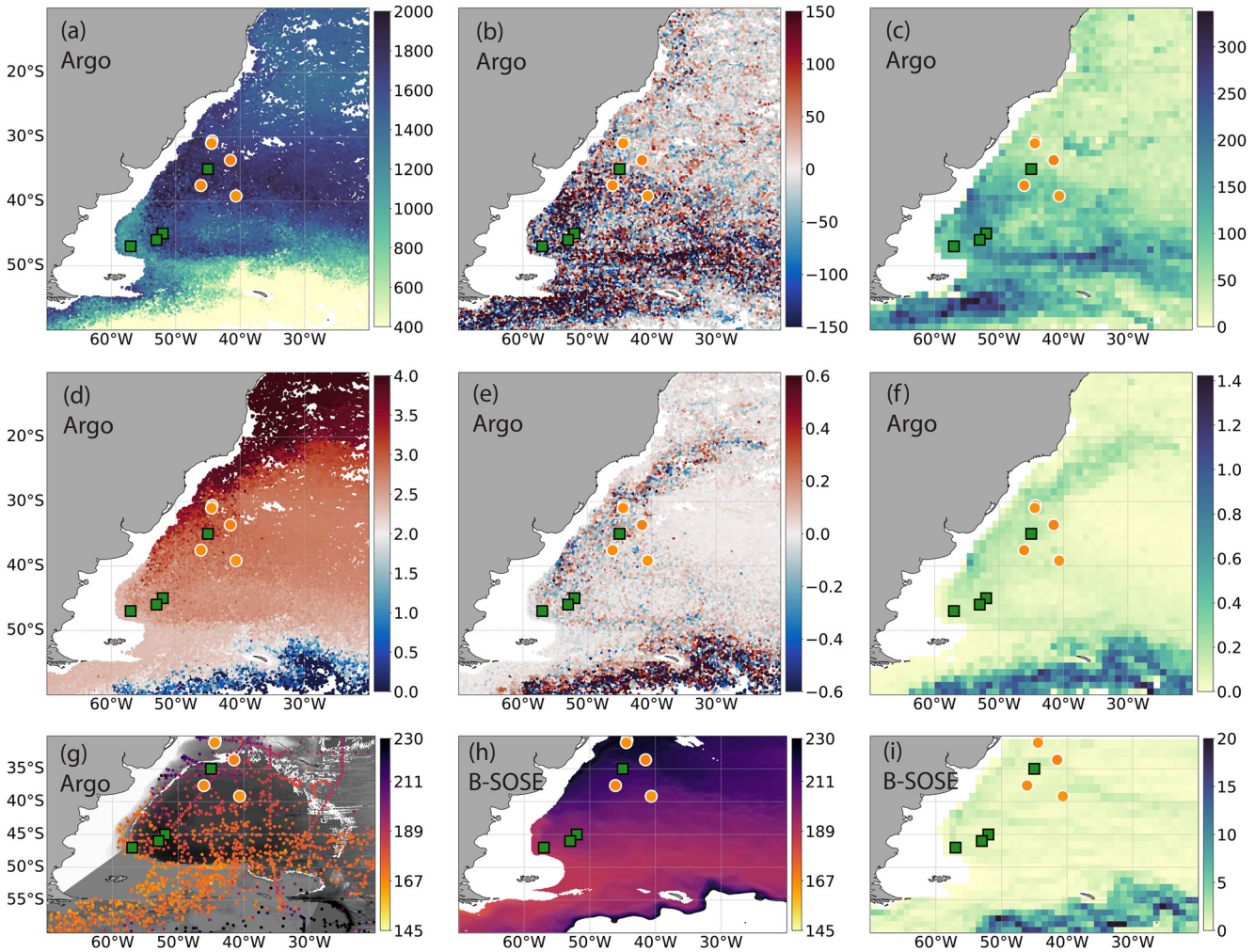

Figure 2. Water properties interpolated on the $\sigma_2 = 36.8$ kg m^{-3} isopycnal. Top row: pressure from Argo profiles (years 1998–2020). (a) Pressure for each profile (dbar), (b) pressure anomaly (dbar) from the 1° × 1° lat/lon bin average for each profile, (c) standard deviation of pressure profiles in 1° × 1° lat/lon bins. Second row: conservative temperature Θ from Argo profiles (years 1998–2020). (d) Θ for each profile (°C), (e) Θ anomaly (°C) from the 1° × 1° lat/lon bin average for each profile, (f) standard deviation of Θ profiles in 1° × 1° lat/lon bins. Third row: dissolved oxygen (μmol/kg). (g) Oxygen from NODC (2005) historical hydrographic station profiles, Southern Ocean Carbon and Climate Observations and Modeling (SOCCOM) Biogeochemical Argo float profiles (years 2015–2021), and quality-controlled oxygen Argo float profiles (Drucker & Riser, 2016), (h) temporally averaged oxygen in 1° × 1° lat/lon bins from the B-SOSE model, (i) standard deviation of oxygen in 1° × 1° lat/lon bins from the B-SOSE model. Locations of profiles with anomalous oxygen in all panels from the three SOCCOM floats (WMOID 5905983, 5905985, and 5905982) are shown as large orange circles colored by dissolved oxygen at $\sigma_2 = 36.8$ kg m^{-3}. Green squares denote historically identified near-bottom eddies.

upwells to the sea surface and acts as a conduit between Northern and Southern Hemisphere polar climates (e.g., Adkins, 2013; Buizert et al., 2015). The admixture of older PDW-dominated CDW thus damps the transmission of Northern climate change to the Southern Ocean.

2. Data and Methods

2.1. Float and Shipboard Profile Data

Our analysis uses in situ measurements from autonomous profiling floats deployed by the Argo and Southern Ocean Carbon and Climate Observations and Modeling (SOCCOM) programs. Core Argo is a global array consisting of approximately 4,000 floats that measure temperature, salinity, and pressure in the upper 2,000 m of the water column every 10 days (Roemmich et al., 2019). Here, we analyze 116,029 delayed-mode, quality-controlled profiles collected in and around the Argentine Basin (60°–10°S, 10°–70°W) from 1998 to 2020. For each profile, we calculate conservative temperature (Θ) (referred to as "temperature" herein), absolute

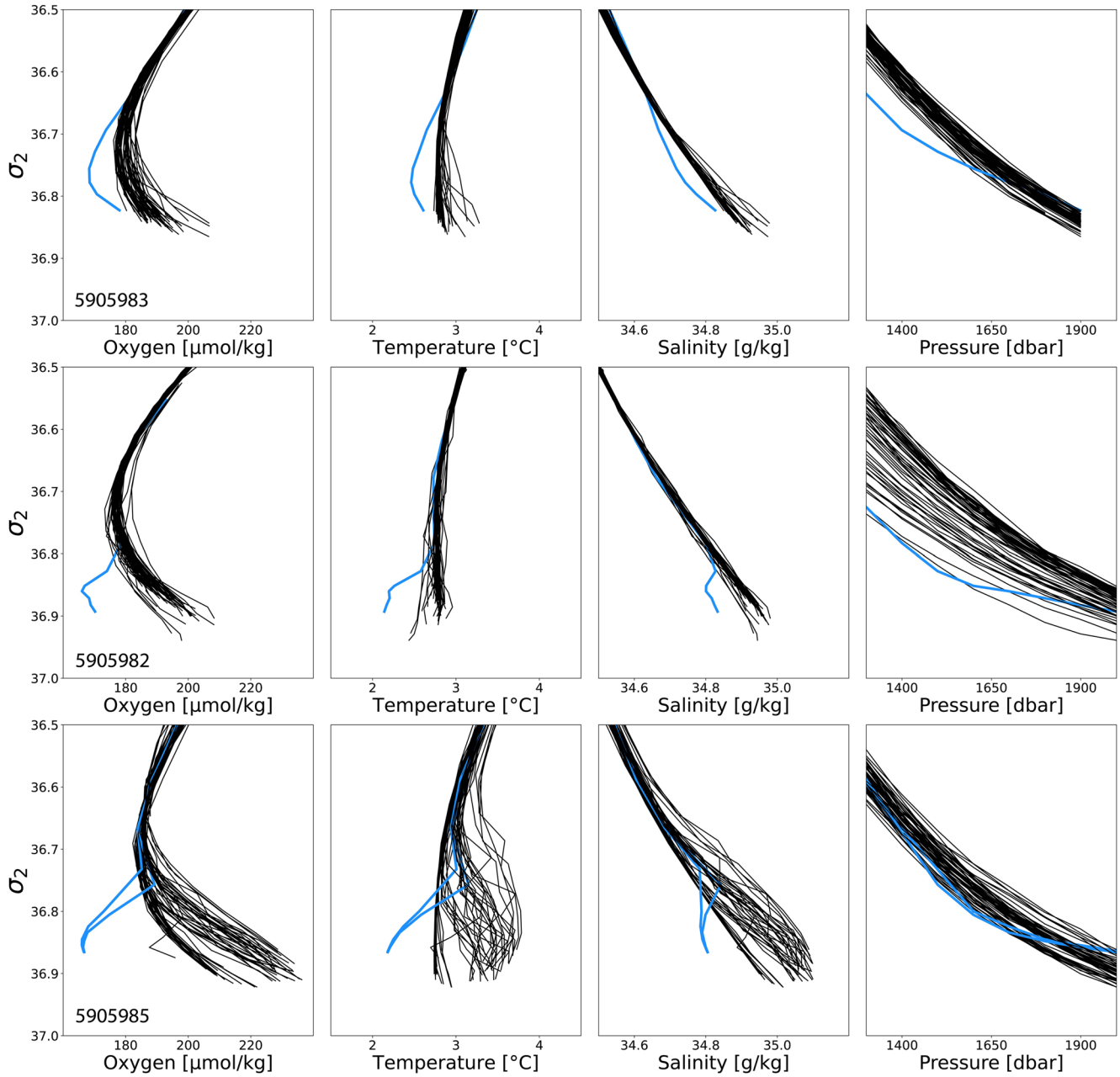

Figure 3. All profiles from the three Southern Ocean Carbon and Climate Observations and Modeling BGC Argo floats with anomalously low oxygen values in the northern Argentine Basin. (Left) Dissolved oxygen, (center left) conservative temperature Θ, (center right) absolute salinity S_A, and (right) pressure profiles from floats 5905983 (top), 5905982 (middle), and 5905985 (bottom). Profiles that are anomalously low in dissolved oxygen relative to the σ_2 = 36.65–36.85 kg m^{-3} isopycnal layer are shown in blue (locations in Figure 2, labeled by float abbreviations shown here in quotes). Profile locations are shown in Supporting Information S1 (Figure S2).

salinity (S_A), and potential density referenced to 2,000 m (σ_2) using the Gibbs seawater (GSW) package routines (http://www.teos-10.org). All fields are then linearly interpolated to a uniformly spaced potential density axis with 0.01 kg m^{-3} resolution. The isopycnal σ_2 = 36.8 kg m^{-3} was selected for most analyses herein, as it characterizes the UCDW oxygen minimum in the Argentine Basin.

SOCCOM has deployed more than 220 Argo-equivalent BGC floats in the Southern Ocean since 2014. SOCCOM floats measure dissolved oxygen, nitrate, pH, fluorescence and backscatter, in addition to temperature and salinity, with the same sampling interval and vertical coverage as core Argo (10 days, 0–2,000 m). The quality-controlled data from the 1 September 2021 SOCCOM snapshot are used in this analysis (Johnson et al., 2021). Here, we

analyze 1118 SOCCOM profiles from 2016 to the present; these include data from 4 floats that were deployed in the Argentine Basin during the 2018 Atlantic Meridional Transect Program (AMT28) (Tarran, 2018) as well as 14 other SOCCOM floats that drifted into the region from the South Pacific or eastern South Atlantic. We also use 206 profiles from 6 non-SOCCOM, oxygen-equipped Argo floats deployed by the University of Washington between 2003 and 2014 (Drucker & Riser, 2016).

In addition to the BGC Argo float data, hydrographic station data are used in Figure 2g to display oxygen at 36.8 σ_2. This curated data set was collated in the early 2000s from Reid's (1994) quality-controlled data sets, augmented by WOCE Hydrographic Program data and other high quality hydrography of the 1980s and 1990s. A total of 610 stations in the Argentine Basin are used here. We also utilize the World Ocean Atlas 2018 dissolved oxygen climatology at 1° × 1° resolution (Garcia et al., 2018) to plot the climatological mean oxygen at 1,500 m (Figure S5 in Supporting Information S1), which is the approximate depth of the 36.8 σ_2 isopycnal (e.g., Figure 2d).

The Biogeochemical Southern Ocean State Estimate (B-SOSE) (Verdy & Mazloff, 2017) is used to identify the inflowing NADW and UCDW transports and properties, and to approximate oxygen statistics, given the much smaller BGC Argo and hydrographic data set compared with the Argo temperature and salinity data set. B-SOSE is a data-assimilating ocean model that constrains the MITgcm solution with multiple observational data sets, including the SOCCOM BGC floats. Iteration 133, with 1/6° resolution, covering years 2013–2018 is used here. Online validation materials show that oxygen in the Argentine Basin at 1,600 m is 10–15 μmol/kg too high, which agrees with our visual comparison (Figures 2g and 2h).

2.2. Argo Temperature and Salinity Anomalies

In Section 3, we present large oxygen anomalies in the deep water density range, observed from SOCCOM profiles, which are also associated with anomalous temperature, salinity, and pressure (Figure 3). To investigate the prevalence of property anomalies with a much larger data set, we compute temperature and salinity statistics using Argo floats. Θ, S_A, and pressure (P) from all Argo profiles flagged as "good" for years 1998–2020 were interpolated to isopycnal surfaces as above. Figure 2a and 2d shows the profile locations, colored by Θ and P on the 36.8 σ_2 level. All fields were then bin-averaged to a 1° × 1° grid (Figure S5 in Supporting Information S1), and for each profile, Θ, S_A, and P anomalies and standard deviations were defined relative to the local bin average (Figure 2). These anomalies highlight locations with significant along-isopycnal variability.

3. UCDW Oxygen Anomalies

The contrast between NADW and CDW is illustrated by oxygen on deep isopycnal and pressure surfaces (Figure 2g; Figures S1, S5 in Supporting Information S1). Namely, low oxygen marks the core of UCDW due to its origin as old Pacific and Indian Deep Water. Salinity also distinctly characterizes NADW and CDW (e.g., Talley, 2013), but the high salinity core of NADW sits below the maximum depth of Argo coverage (i.e., 2,000 m). In the Argentine Basin, higher oxygen concentrations occur at the western boundary where NADW penetrates southward. The lowest oxygen values are observed in the southern Argentine Basin, where UCDW crosses the Falkland Plateau in both the Subantarctic and Polar Fronts (Figure 1).

The oxygen climatology at 1,500 m (Figure S5c in Supporting Information S1) shows concentrations between 180 and 200 μmol/kg throughout the Argentine Basin, except in the northern DWBC where it is higher. However, this smoothed field obscures significant deep variability. For example, south of the Brazil-Malvinas Confluence (BMC) at 40°S, the individual hydrographic station profiles at 36.8 σ_2 (Figure 2g) reveal lower oxygen in the Malvinas with patchy higher oxygen offshore where Brazil Current water extends toward Zapiola Rise (Figure 1). North of the BMC, isolated profiles of higher oxygen (purple) suggest southward movement of NADW along the western boundary, while isolated profiles of lower oxygen (lighter orange) indicate penetration of UCDW as far north as 37°S at the western boundary and 30°S offshore.

SOCCOM BGC floats, for example, recorded remarkably low dissolved oxygen concentration in the UCDW range (σ_2 = 36.65–36.9) in the northern Argentine Basin (5 large orange dots in Figure 1; Figure 3). Their oxygen concentrations ranged from 12 to 52 μmol/kg lower than the other profiles measured by these floats, which is 2–8 times the standard deviation (Figures 2 and 3; Table S1 in Supporting Information S1). These extreme oxygen anomalies were also associated with anomalously low temperature and salinity (Figure 3), and high nitrate and

low pH (Figure S3 in Supporting Information S1), and thus are unlikely to be due to sensor malfunction. Each anomaly has a striking vertical structure, with an abrupt break in the profile at the top of the anomaly in physical space, occurring between 1,000 and 1,700 m, and at densities of σ_2 = 36.6–36.8. Note that because Argo profiles are limited to 2,000 m, the bottoms of the anomalies cannot be characterized.

The density, oxygen concentration, and Θ of these anomalies are consistent with UCDW, whose principal source in the Argentine Basin is the southeast Pacific Ocean's oxygen-poor PDW. PDW enters the Atlantic through Drake Passage and then follows the Malvinas Current northward (Figure S1 in Supporting Information S1). Circulation schematics often feature an anticyclonic pathway of CDW around the Argentine Basin (e.g., Stramma & England, 1999; Valla et al., 2018), following the dominant route for the overlying AAIW (Reid, 1989). However, CDW is constantly mixing with ambient waters along this pathway and thus would be strongly modified along such a circuitous route to the northwestern Argentine Basin where the anomalous profiles were found. Therefore, the anomalies most likely moved directly northeastward from the BMC. This is supported by Reid's (1989, 1994) circulation at 1,500–2,500 m and Valla et al.'s (2018) hydrographic data analysis at 34.5°S, and is the basis for our Figure 1 schematic.

The unusual abrupt vertical layering of northern and southern water masses in these anomalous profiles indicates relatively pure sources of each. To reach the location of the northernmost anomalies, pristine oxygen-poor CDW must propagate 500–1,000 km from its nearest source at the BMC, and twice that distance from entry at the Falkland Plateau. This could be accomplished by coherent subthermocline eddies, which do not easily mix with surrounding water. The abruptness of the anomalous profile breaks indicates local layering/intrusions. However, the layer breaks are not at uniform depths or densities (~1,300–1,600 m depth, Figure 3). This suggests bathymetry-following southward flow of NADW that is forced offshore by the topography and then into or over eddies containing purer CDW. Indeed, float 5905982 followed just such a pathway offshore from the Brazil Current into an eddying field (Figure S2b in Supporting Information S1), and notably recorded 3 of the 5 SOCCOM low oxygen anomalies.

Given that we only have single profiles, we cannot unequivocally say that the oxygen anomalies are due to coherent subthermocline vortices, although they are associated with small negative pressure anomalies (Figure 3), suggesting that they are cyclonic. Likely relevant to identification as vortices, Gordon and Greengrove (1986) and Arhan et al. (2002) have previously documented much deeper subthermocline eddies containing the denser LCDW in the Argentine Basin (green squares in Figure 2), using tightly spaced hydrographic stations. Arhan et al. (2002) hypothesized that these deep eddies originated from destabilization of the deep Malvinas Current at a point along the Malvinas Loop. The northernmost eddy identified by Arhan et al. (2002) is co-located with the northern cluster of SOCCOM oxygen anomalies.

In addition to the 5 anomalous oxygen profiles discussed above, several other prominent layered anomalies were observed in the southern Argentine Basin (Figure 1; Table S2 in Supporting Information S1). For example, multiple low oxygen anomalies in the eastward flow between Zapiola Rise and the Falkland Escarpment likely resulted from the movement of UCDW across the Falkland Plateau with the Polar Front. These contribute to UCDW/NADW mixing along the Subantarctic Front, but are unlikely to circulate northwestward into the northern Argentine Basin. Several high oxygen anomalies (Figure 1; Figure S4 in Supporting Information S1) were located in the BMC, where NADW and UCDW meet head-on. Finally, a high oxygen anomaly, which would be NADW from the Brazil Current, was found southwest of Zapiola Rise (Figure S4c in Supporting Information S1), where historical oxygen data also suggest such anomalies (Figure 2g).

Profiles with these anomalous layered structures are relatively rare, constituting only a handful of the total 1118 SOCCOM BGC profiles in the Argentine Basin. This is perhaps surprising given how eddy-rich the region is (Juillon et al., 2010; Piola & Matano, 2017), suggesting that the energetic mixing between water masses proceeds at the smaller vertical fine structure scales of 10–100 m (Bianchi et al., 1993; Georgi, 1981).

4. Deep Water Eddy Field

The notable but rare anomalies reported in Section 3 are due to interleaving of NADW and UCDW in the circulation and eddy field of the Argentine Basin (Georgi, 1981). Since the oxygen anomalies are also associated with anomalous temperature and salinity (Figure 3), we turn to the much larger Argo temperature-salinity data set for a more comprehensive view of the water mass juxtaposition. As described in Section 2.2, we interpolated Θ,

S_A, and P onto isopycnal surfaces, focusing analysis on the 36.8 σ_2 surface, which lies in the core of the UCDW oxygen minimum layer. By "NADW" for this isopycnal, we refer to the warm, salty, oxygenated water originating from the north, but which lies above the NADW core's salinity maximum that is below the Argo depth range of 2,000 m. We then bin average Θ and P (Figure S5 in Supporting Information S1), and calculate the anomaly for each profile relative to the local mean in each bin.

The conservative temperature, Θ, distribution at 36.8 σ_2 (Figure 2d; Figure S5 in Supporting Information S1) has a strong meridional gradient. Namely, warm NADW from the north enters the Argentine Basin in the DWBC, while cool UCDW from Drake Passage crosses the Falkland Plateau and flows equatorward in the Malvinas Current. Other polar waters cross the Falkland Escarpment farther to the east (Figure 1), but proceed eastward and mostly out of the domain. The pressure at 36.8 σ_2 (Figure 2a; Figure S5a in Supporting Information S1) is 1,200–1,800 dbar in the Argentine and Brazil Basins. Note that the isopycnal rises steeply southward across the Polar Front indicating outcropping within the ACC; however this outcropped water has limited impact on Argentine Basin UCDW. Within the Argentine Basin, the subtler patterns of Θ and P variability at 36.8 σ_2 (Figures 2b and 2e) are relevant to the extreme oxygen anomalies. Just after the warm DWBC moves southward past Sao Paulo Plateau, it spawns an eastward excursion of warmer water around 33°S. The 3 northernmost extreme oxygen anomalies (orange circles) are located in this eastward plume.

Regions with significant along-isopycnal variability are marked by large anomalies and standard deviations relative to the local bin average (Figure 2). A band of the largest Θ anomalies and standard deviations (Figures 2e and 2f) forms a striking pattern along the offshore side of the warm western boundary waters. This is the mixing front (water mass front) between NADW and UCDW. Hotspots of anomalies appear at 40°S in the BMC, and at the entry location of the DWBC to the Argentine Basin over the Sao Paulo Plateau. (Farther north in the Brazil Basin, the strong anomalies extend eastward in a band around 20°–25°S, marking the local eastward flow of NADW from the DWBC) Standard deviation of Θ within the 1° × 1° bins (Figure 2f) also highlights the high variability along the water mass front and at the BMC.

Large isopycnic temperature anomalies result from both a large water mass contrast and a dynamic eddy field. The eddy field, in turn, is represented by isopycnic P anomalies (Figure 2b), which indicate locations with significant vertical excursions of the isopycnal. The highest P anomalies are found at the western boundary in the Malvinas and DWBC, and along the Falkland Escarpment to the south. High P variability also occurs where the Brazil and Malvinas Current fronts split around Zapiola Rise (Figure 1 schematic based on Reid, 1989), and to the east of the Rise where these flows rejoin. This overall deep pattern, of a "donut" of high variability in the Argentine Basin, with weak variability over Zapiola Rise and in the Brazil Basin, strongly resembles surface eddy kinetic energy from altimetry (e.g., Mason et al., 2017; Yu et al., 2018).

It is important to realize that large P and Θ anomalies are not necessarily co-located. In other words, dynamical and water mass variability patterns differ (Figures 2b and 2d). Along-isopycnal Θ variability in the Argentine Basin is highest along the western boundary where there is both a UCDW/NADW water mass front and high pressure variability. However, in the zonal portions of the Argentine Basin's "donut" of high pressure variability and thus high eddy activity, temperature variability is low because of the absence of a water mass contrast. This contrast was also noted in Valla et al. (2018) with respect to the northwest Argentine Basin. Finally, even farther north, Θ variability is high in the southern Brazil Basin, where there is a strong zonal CDW/NADW boundary (Figure 2d) but little pressure variability (Figure 2a).

Mixing between NADW and UCDW can be related to these variability distributions. We apply a simple end-member mixing calculation on the isopycnal σ_2 = 36.8 kg m^{-3} with two sources: warm Brazil Current NADW at 30°S and cool Malvinas Current UCDW at 50°S. Transports in B-SOSE were used to identify the inflow longitudes (Text S3 in Supporting Information S1). The reference Θ and S_A at 36.8 σ_2 were (3.28°C, 34.93 g/kg) for NADW and (2.38°C, 34.76 g/kg) for UCDW, based on B-SOSE time averages and verified with averaged Argo data in the same locations. The end-member calculation was applied to the 1° × 1° bin-averaged Argo profiles (Figures S7a, S7c in Supporting Information S1) and to B-SOSE (Text S3, Figure S8 in Supporting Information S1). We found a larger eastward extension of warmer NADW in B-SOSE compared with Argo, along with a similar feature in B-SOSE's oxygen distribution that is not matched in observations (Figures 2g and 2h), which suggests that the model's eddy variability relative to advection is weaker than in the real ocean (e.g., Swierczek et al., 2021). Therefore, we focus on the Argo analysis here.

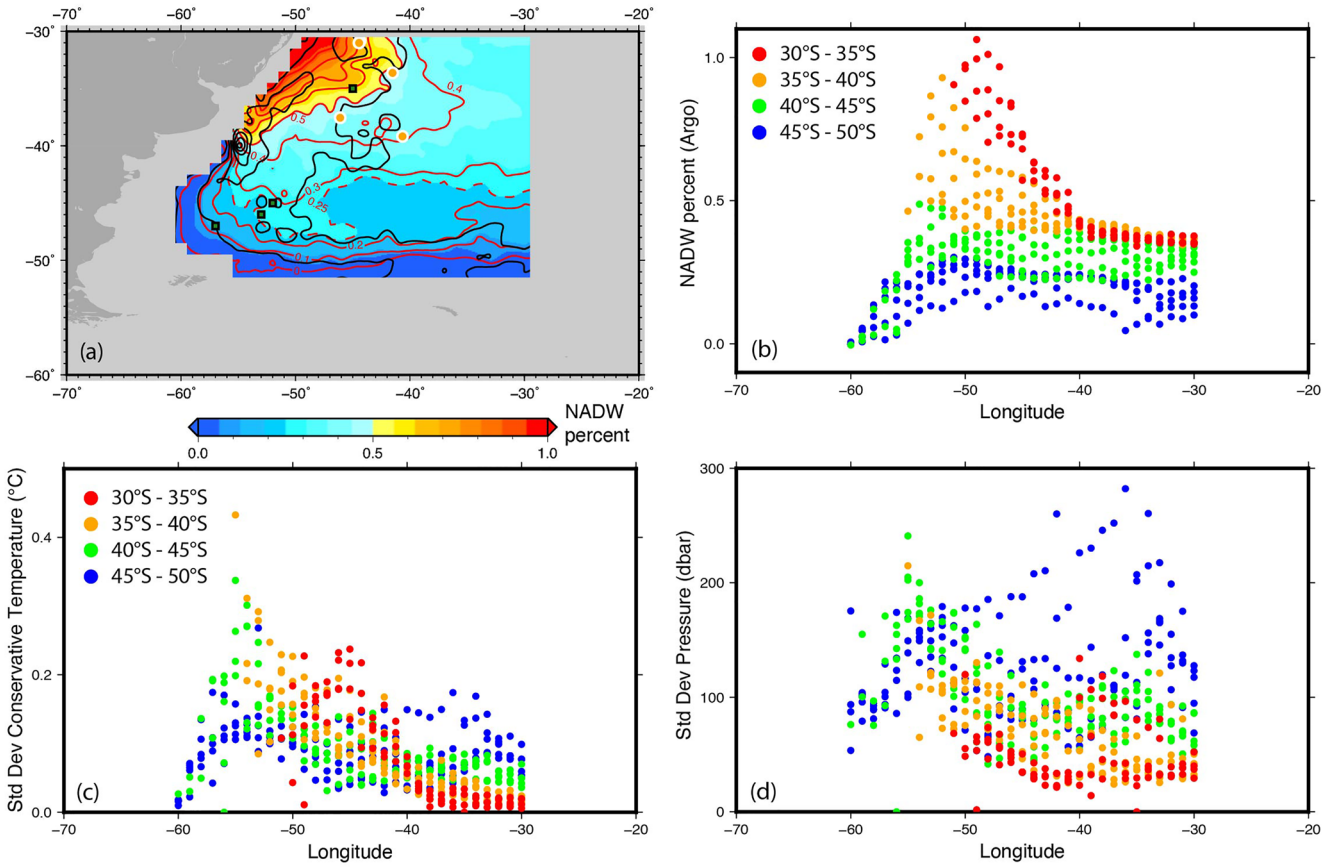

Figure 4. (a) North Atlantic Deep Water (NADW) fraction (color and red contours) at $\sigma_2 = 36.8$ kg m^{-3}, assuming two end-member mixing between NADW and Upper Circumpolar Deep Water, using 1° × 1° binned averages from Argo profiles. Black contours are Θ standard deviation. Locations of anomalous oxygen profiles (orange dots) and previous deep eddies (green) as in Figure 2. (b) Fraction of NADW. (c) Standard deviation of Θ (°C). (d) Standard deviation of pressure. Colored by latitude ranges: 30°–35°S (orange), 35°–40°S (red), 40°–45°S (green), 45°–50°S (blue).

Highest NADW fractions relative to UCDW (Figures 4a and 4b) occur in the Brazil Current, which is surrounded by a 0.5 NADW contour. A region of high Θ standard deviation extends about 700 km offshore along the entire western boundary, and is highest at the BMC at 40°S. The 0.5 NADW contour ends at the BMC, and the presumption is that all Brazil Current water moving eastward from this point has undergone mixing. Between Rio Grande Rise and 35°S, the 0.4 NADW contour bulges eastward. Our 5 anomalous oxygen profiles (Figure 3) are in this region, suggesting interaction between northward-flowing Malvinas water and southward-flowing Brazil Current water, with both eddying eastward offshore.

Both the NADW fraction and Θ standard deviation transition to more uniform values east of 40°W (Figure 4c). Here the fraction of NADW is about 0.37 for 30°–40°S, which lies north of the BMC eastward extension and east of the "bulge." Lower percentages occur south of this, where the Malvinas UCDW influence is larger: 0.25 –0.35 for 40°–45°S, and 0.1–0.25 for 45°–50°S (Figure 4c). The overall lower fraction of NADW relative to UCDW throughout most of the Argentine Basin can be accounted for by the lower Brazil Current inflow transport relative to the Malvinas in the deep water range.

Note that pressure variability remains high east of about 43°W (Figure 4d). Hence, the low Θ variability suggests that most property mixing has occurred by this point despite the dynamically active eddy field.

5. Conclusions

In discussions of the meridional overturning circulation (MOC), the focus is usually on the fate of the ventilated, sinking components from the Northern Hemisphere that produce NADW and from the Southern Hemisphere that produce AABW/LCDW. These carry the history of surface conditions from their formation regions to the

upwelling regions of the global ocean, mostly within the ACC and to its south. Often lost in this simplified view of the MOC is the modification of these waters, particularly NADW, as they traverse their overturning pathways. Once NADW leaves the mid-latitude North Atlantic and is advected southward, its properties are mostly maintained until it reaches the mid-latitude South Atlantic. Previous studies have shown that almost 80% of the southward NADW transport goes through the Argentine Basin (Garzoli et al., 2015), a region with significant deep and abyssal variability (Kersale et al., 2020). We note though that the high salinity, high oxygen signature of NADW weakens almost immediately upon entry into the region near the Sao Paulo Plateau at about 30°S (Figure 1). As the NADW flows further southward in the Argentine Basin, it is further modified until it encounters the Brazil-Malvinas Confluence (Figures 1, 2, and 4). The modified NADW turns to flow eastward both north and south of Zapiola Rise and then joins the eastward circumpolar flow.

This significant modification of NADW in the Argentine Basin is due to mixing with CDW, both at the depth of the NADW core and sandwiching it above and below. We have shown, using the sparse BGC Argo data set, augmented with historical hydrographic data, that nearly unadulterated CDW is found sporadically in the northwestern Argentine Basin. These extreme, isolated oxygen anomalies substantiate an important pathway northward from the BMC (Valla et al., 2018), rather than the more circuitous counterclockwise path around the full South Atlantic depicted in many previous schematics. Moreover, these isolated anomalies are located where we have shown that temperature/salinity variability is large on NADW/CDW isopycnals, based on the larger core Argo data set. Hence the primary mixing interface between NADW and CDW is within the western boundary currents. Notably, a strong eddy field is a necessary condition for mixing of the water masses, but it is not sufficient—strong dilution of NADW also requires the water mass contrast created by the northward shortcut of CDW in this western region.

Why is it important to document mixing between deep waters? When NADW enters the Southern Ocean, its properties are informed by surface processes in the northern North Atlantic about 200 years earlier, as well as the modification that occurs through mixing as these waters traverse the length of the Atlantic. This modification is most extreme in the Argentine Basin due to CDW, whose low oxygen, high carbon, and low pH (e.g., Figure S3 in Supporting Information S1) result from its aged components; PDW age exceeds 1,000 years. These time scales could lead to higher carbon outgassing potential in PDW/CDW than in NADW (Chen et al., 2022). But by the time NADW enters the Southern Ocean and upwells to the sea surface, it has been diluted by mixing with carbon-rich CDW, and therefore is nearly equally capable of outgassing at the sea surface (Bushinsky et al., 2019; Prend et al., 2022). If the dilution rate depends on fluctuations in the Malvinas and Brazil/Deep Western Boundary Current transports and eddy fields, then changes in forcing on climatic time scales could alter the properties of the upwelled deep waters and associated air-sea gas exchange.

Here we have seen that the expanding BGC float sampling of the western South Atlantic, almost equal in just 3 years to the historical ship-based data set, is revealing deep water property anomalies that clarify understanding of the juxtaposition and mixing of the globally important CDW and NADW. The 17 years of Argo profiling in the same region provides a comprehensive geographic view of the mixing of these deep waters. Both reveal the importance of the western boundary region of the Argentine Basin for southward and northward transport. The expected continued BGC float sampling in the subtropical South Atlantic will eventually allow dense mapping of BGC anomalies similar to the temperature/salinity fields, and hence improved quantification of BGC property dilution as it reaches the Southern Ocean.

Data Availability Statement

BGC profiling float data were collected and made freely available by the Southern Ocean Carbon and Climate Observations and Modeling (SOCCOM) Project funded by the National Science Foundation, Division of Polar Programs (NSF PLR -1425989), supplemented by NASA, and by the International Argo Program and the NOAA programs that contribute to it (http://www.argo.ucsd.edu, http://argo.jcommops.org). The Argo Program is part of the Global Ocean Observing System. All SOCCOM data are available through the Argo GDACs. Calibrated SOCCOM data from the 20 April 2020 snapshot (https://doi.org/10.6075/J0KK996D) were used here, which is available at https://soccompu.princeton.edu/www/index.html. The calibrated Argo oxygen data from Drucker and Riser (2016) are available at https://soccom.princeton.edu/content/uw-global-o2-data-set; these data are also part of the complete Argo data set, as above. Shipboard hydrographic data were collected by the World Ocean Circulation Experiment (WOCE) and numerous other selected research cruises spanning many decades. All data are

available from the NCEI World Ocean Database (WOD) (https://www.ncei.noaa.gov/access/world-ocean-database-select/dbsearch.html) and were quality controlled by J. L. Reid (Reid, 1994) and co-author LDT. The oxygen climatology based on historical hydrographic data is from the World Ocean Atlas 2018 (Garcia et al., 2018), and is available at https://www.ncei.noaa.gov/access/world-ocean-atlas-2018/. The B-SOSE data was from the Iteration 133 solution (Verdy and Mazloff, 2017). B-SOSE is a contribution of the SOCCOM Project, and data from the 133 iteration can be found at http://sose.ucsd.edu/BSOSE6_iter133_solution.html.

Acknowledgments
We acknowledge our SOCCOM program colleagues for production of BGC floats, B-SOSE and data processing since 2014, and for years of scientific discussion. We thank G. Tarran and the science party of Plymouth Marine Laboratory for deploying the Argentine Basin SOCCOM floats during the AMT28 project on the RRS James Clark Ross (https://www.amt-uk.org/Cruises/AMT28). SVSB, LDT and CJP were supported by NSF PLR-1425989 and OPP-1936222 to the SOCCOM program. CJP was also supported by a National Science Foundation Graduate Research Fellowship under Grant DGE-1650112.

References

Adkins, J. (2013). The role of deep ocean circulation in glacial to interglacial climate change. *Paleoceanography*, *28*, 1–23. https://doi.org/10.1002/palo.20046

Arhan, M., Carton, X., Piola, A., & Zenk, W. (2002). Deep lenses of circumpolar water in the Argentine Basin. *Journal of Geophysical Research*, *107*(C1), 7–1. https://doi.org/10.1029/2001jc000963

Bianchi, A. J., Giulivi, C. F., & Piola, A. R. (1993). Mixing in the Brazil-Malvinas confluence. *Deep-Sea Research* I, *40*(7), 1345–1358. https://doi.org/10.1016/0967-0637(93)90115-j

Buizert, C., Adrian, B., Ahn, J., Albert, M., Alley, R. B., Baggenstos, D., & Woodruff, T. E. (2015). Precise interpolar phasing of abrupt climate change during the last ice age. *Nature*, *520*(7549), 661–665. https://doi.org/10.1038/nature14401

Bushinsky, S. M., Landschutzer, P., Rodenbeck, C., Gray, A. R., Baker, D., Mazloff, M. R., et al. (2019). Reassessing Southern Ocean air-sea CO_2 flux estimates with the addition of biogeochemical float observations. *Global Biogeochemical Cycles*, *33*, 1370–1388. https://doi.org/10.1029/2019GB006176

Chen, H., Haumann, F. A., Talley, L. D., Johnson, K. S., & Sarmiento, J. (2022). The deep ocean's carbon exhaust. *Global Biogeochemical Cycles*, *36*, e2021GB007156. https://doi.org/10.1029/2021GB007156

Drucker, R., & Riser, S. C. (2016). In situ phase-domain calibration of oxygen Optodes on profiling floats. *Methods in Oceanography*, *17*, 296–318. https://doi.org/10.1016/j.mio.2016.09.007

Ganachaud, A., & Wunsch, C. (2000). Improved estimates of global ocean circulation, heat transport and mixing from hydrographic data. *Nature*, *408*(6811), 453–457. https://doi.org/10.1038/35044048

Garcia, H. E., Weathers, K., Paver, C. R., Smolyar, I., Boyer, T. P., Locarnini, R. A., et al. (2018). World Ocean Atlas 2018, volume 3: Dissolved oxygen, apparent oxygen utilization, and oxygen saturation. In A. Mishonov (Ed.), Technical Ed, *NOAA Atlas NESDIS* (Vol. *83*, p. 38).

Garzoli, S. L., Dong, S., Fine, R., Meinen, C. S., Perez, R. C., Schmid, C., et al. (2015). The fate of the deep western boundary current in the South Atlantic. Deep sea research Part A. *Oceanographic Research Papers*, *103*, 125–136. https://doi.org/10.1016/j.dsr.2015.05.008

Garzoli, S. L., & Matano, R. (2011). The South Atlantic and the Atlantic meridional overturning circulation. *Deep Sea Research Part II: Topical Studies in Oceanography*, *58*(17–18), 1837–1847.

Georgi, D. T. (1981). On the relationship between the large-scale property variations and fine structure in the Circumpolar Deep Water. *Journal of Geophysical Research*, *86*(C7), 6556–6566. https://doi.org/10.1029/jc086ic07p06556

Gordon, A. L., & Greengrove, C. L. (1986). Geostrophic circulation of the Brazil-Falkland confluence. Deep sea research Part A. *Oceanographic Research Papers*, *33*(5), 573–585. https://doi.org/10.1016/0198-0149(86)90054-3

Hernández-Guerra, A., Talley, L. D., Pelegrí, J. L., Vélez-Belchí, P., Baringer, M. O., Macdonald, A. M., & McDonagh, E. L. (2019). The upper, deep, abyssal and overturning circulation in the Atlantic Ocean at 30°S in 2003 and 2011. *Progress in Oceanography*, *176*, 102136. https://doi.org/10.1016/j.pocean.2019.102136

Johnson, K. S., Riser, S. C., Boss, E. S., Talley, L. D., Sarmiento, J. L., Swift, D. D., et al. (2021). SOCCOM float data—Snapshot 2021-09-21. In *Southern Ocean Carbon and Climate Observations and Modeling (SOCCOM) float data archive*. UC San Diego Library Digital Collections. https://doi.org/10.6075/J0CF9Q81

Jullion, L., Heywood, K. J., Naveira Garabato, A. C., & Stevens, D. P. (2010). Circulation and water mass modification in the Brazil–Malvinas confluence. *Journal of Physical Oceanography*, *40*(5), 845–864. https://doi.org/10.1175/2009jpo4174.1

Kersale, M., Meinen, C. S., Perez, R. C., Le Henaff, M., Valla, D., Lamont, T., et al. (2020). Highly variable upper and abyssal overturning cells in the South Atlantic. *Science Advances*, *6*(32), eaba7573. https://doi.org/10.1126/sciadv.aba7573

Lumpkin, R., & Speer, K. (2007). Global Ocean meridional overturning. *Journal of Physical Oceanography*, *37*(10), 2550–2562. https://doi.org/10.1175/jpo3130.1

Mason, E., Pascual, A., Gaube, P., Ruiz, S., Pelegrí, J. L., & Delepoulle, A. (2017). Subregional characterization of mesoscale eddies across the Brazil-Malvinas confluence. *Journal of Geophysical Research: Oceans*, *122*(4), 3329–3357. https://doi.org/10.1002/2016JC012611

McCarthy, G. D., Smeed, D. A., Johns, W. E., Frajka-Williams, E., Moat, B. I., Rayner, D., et al. (2015). Measuring the Atlantic meridional overturning circulation at 26°N. *Progress in Oceanography*, *130*, 91–111. https://doi.org/10.1016/j.pocean.2014.10.006

McCartney, M. S. (1992). Recirculating components to the deep boundary current of the northern North Atlantic. *Progress in Oceanography*, *29*(4), 283–383. https://doi.org/10.1016/0079-6611(92)90006-l

NODC. (2005). *World ocean database 2005 (WOD05)*. NOAA National Oceanographic Data Center. Retrieved from http://www.nodc.noaa.gov/OC5/WOD05/pr_wod05.html

Piola, A. R., & Gordon, A. L. (1989). Intermediate waters in the southwest South Atlantic. *Deep Sea Research I*, *36*, 1–16. https://doi.org/10.1016/0198-0149(89)90015-0

Piola, A. R., & Matano, R. P. (2017). Ocean currents: Atlantic western boundary—Brazil current/Falkland (Malvinas) current. In *Encyclopedia of ocean sciences (Third Edition). Reference module in earth systems and environmental sciences*. Elsevier. https://doi.org/10.1016/B978-0-12-409548-9.10541-X

Prend, C. J., Gray, A. R., Talley, L. D., Gille, S. T., Haumann, F. A., Johnson, K. S., et al. (2022). Indo-Pacific sector dominates Southern Ocean carbon outgassing. *Global Biogeochemical Cycles*, *36*(7), e2021GB007226. https://doi.org/10.1029/2021gb007226

Reid, J. L. (1989). On the total geostrophic circulation of the South Atlantic Ocean: Flow patterns, tracers and transports. *Progress in Oceanography*, *23*(3), 149–244. https://doi.org/10.1016/0079-6611(89)90001-3

Reid, J. L. (1994). On the total geostrophic circulation of the North Atlantic Ocean: Flow patterns, tracers and transports. *Progress in Oceanography*, *33*, 1–92. https://doi.org/10.1016/0079-6611(94)90014-0

Reid, J. L., Nowlin, W. D., & Patzert, W. C. (1977). On the characteristics and circulation of the southwestern Atlantic Ocean. *Journal of Physical Oceanography*, *7*(1), 62–91. https://doi.org/10.1175/1520-0485(1977)007<0062:otcaco>2.0.co;2

Rhein, M., Kieke, D., & Steinfeldt, R. (2015). Advection of North Atlantic deep water from the Labrador Sea to the southern hemisphere. *Journal of Geophysical Research: Oceans*, *120*(4), 2471–2487. https://doi.org/10.1002/2014JC010605

Roemmich, D., Alford, M. H., Claustre, H., Johnson, K., King, B., Moum, J., et al. (2019). On the future of Argo: A global, full-depth, multi-disciplinary array. *Frontiers in Marine Science*, *6*, 439. https://doi.org/10.3389/fmars.2019.00439

Schmitz, W. J. (1995). On the interbasin-scale thermohaline circulation. *Reviews of Geophysics*, *33*(2), 151–173. https://doi.org/10.1029/95rg00879

Stramma, L., & England, M. (1999). On the water masses and mean circulation of the South Atlantic Ocean. *Journal of Geophysical Research*, *104*(C9), 20863–20883. https://doi.org/10.1029/1999jc900139

Swierczek, S., Mazloff, M. R., Morzfeld, M., & Russell, J. L. (2021). The effect of resolution on vertical heat and carbon transports in a regional ocean circulation model of the Argentine Basin. *Journal of Geophysical Research: Oceans*, *126*(7), e2021JC017235. https://doi.org/10.1029/2021jc017235

Talley, L. D. (2013). Closure of the global overturning circulation through the Indian, Pacific, and Southern Oceans: Schematics and transports. *Oceanography*, *26*(1), 80–97. https://doi.org/10.5670/oceanog.2013.07

Talley, L. D., Pickard, G. L., Emery, W. J., & Swift, J. H. (2011). *Descriptive physical oceanography: An introduction* (6th ed., p. 560), Elsevier.

Talley, L. D., Reid, J. L., & Robbins, P. E. (2003). Data-based meridional overturning streamfunctions for the global ocean. *Journal of Climate*, *16*(19), 3213–3226. https://doi.org/10.1175/1520-0442(2003)016<3213:dmosft>2.0.co;2

Tamsitt, V., Drake, H., Morrison, A. K., Talley, L. D., Dufour, C. O., Gray, A. R., et al. (2017). Spiraling up: Pathways of global deep waters to the surface of the Southern Ocean. *Nature Communications*, *8*(1), 172. https://doi.org/10.1038/s41467-017-00197-0

Tarran, G. (2018). *AMT 28 cruise report: RRS James Clark Ross (JR18-001)*. Atlantic Meridional Transit Project Office, Plymouth Marine Laboratory. Retrieved from https://www.amt-uk.org/getattachment/Cruises/AMT28/AMT_28_CRUISE_REPORT_RS.pdf

Valla, D., Piola, A. R., Meinen, C. S., & Campos, E. (2018). Strong mixing and recirculation in the northwestern Argentine Basin. *Journal of Geophysical Research: Oceans*, *123*(7), 4624–4648. https://doi.org/10.1029/2018jc013907

Verdy, A., & Mazloff, M. R. (2017). A data assimilating model for estimating Southern Ocean biogeochemistry. *Journal of Geophysical Research: Oceans*, *122*(9), 69686988–6988. https://doi.org/10.1002/2016JC012650

Wüst, G. (1935). Schichtung und Zirkulation des Atlantischen Ozeans. Die Stratosphäre. In Wissenschaftliche Ergebnisse der Deutschen Atlantischen Expedition auf dem Forschungs- und Vermessungsschiff "Meteor" 1925-1927. *61st Part*, *2*, 109–288. (in German).

Yu, Y., Chao, B. F., García-García, D., & Luo, Z. (2018). Variations of the Argentine Gyre observed in the GRACE time-variable gravity and ocean altimetry measurements. *Journal of Geophysical Research: Oceans*, *123*(8), 5375–5387. https://doi.org/10.1029/2018jc014189

References From the Supporting Information

Beal, L., De Ruijter, W., Biastoch, A., Zahn, R., Cronin, M., Hermes, J., et al. (2011). On the role of the Agulhas system in ocean circulation and climate. *Nature*, *472*(7344), 429–436. https://doi.org/10.1038/nature09983

Koltermann, K. P., Gouretski, V. V., & Jancke, K. (2011). *Hydrographic Atlas of the world ocean circulation experiment (WOCE). Volume 3: Atlantic Ocean*. In M. Sparrow, P. Chapman, & J. Gould (Eds.). International WOCE Project Office. ISBN 090417557X Retrieved from http://woceatlas.ucsd.edu/index.html